Cellular NH_4^+/K^+ Transport Pathways in Mouse Medullary Thick Limb of Henle

Regulation by Intracellular pH

DEEPAK KIKERI, ADAM SUN, MARK L. ZEIDEL, and STEVEN C. HEBERT

From the Harvard Center for the Study of Kidney Disease, Harvard Medical School, and Laboratory of Molecular Physiology and Biophysics, Renal Division, Brigham & Women's Hospital, Boston, Massachusetts 02115; and Renal Section, Medical Service, Veterans Administration Hospital, West Roxbury, Massachusetts 02132

ABSTRACT Fluorescence and electrophysiological methods were used to determine the effects of intracellular pH (pH_i) on cellular NH_4^+/K^+ transport pathways in the renal medullary thick ascending limb of Henle (MTAL) from CD1 mice. Studies were performed in suspensions of MTAL tubules (S-MTAL) and in isolated, perfused MTAL segments (IP-MTAL). Steady-state pH_i measured using 2,7-biscarboxyethyl-5(6)-carboxyfluorescein (BCECF) averaged 7.42 ± 0.02 (mean ± SE) in S-MTAL and 7.26 ± 0.04 in IP-MTAL. The intrinsic cellular buffering power of MTAL cells was 29.7 ± 2.4 mM/pH_i unit at pH_i values between 7.0 and 7.6, but below a pH_i of 7.0 the intrinsic buffering power increased linearly to ~50 mM/pH_i unit at pH_i 6.5. In IP-MTAL, NH_4^+ entered cells across apical membranes via both Ba^{2+}-sensitive pathway and furosemide-sensitive $Na^+:K^+(NH_4^+):2Cl^-$ cotransport mechanisms. The $K_{0.5}$ and maximal rate for combined apical entry were 0.5 mM and 83.3 mM/min, respectively. The apical Ba^{2+}-sensitive cell conductance in IP-MTAL (G_c), which reflects the apical K^+ conductance, was sensitive to pH_i over a pH_i range of 6.0–7.4 with an apparent $K_{0.5}$ at pH_i ~6.7. The rate of cellular NH_4^+ influx in IP-MTAL due to the apical Ba^{2+}-sensitive NH_4^+ transport pathway was sensitive to reduction in cytosolic pH whether pH_i was changed by acidifying the basolateral medium or by inhibition of the apical $Na^+:H^+$ exchanger with amiloride at a constant pH_o of 7.4. The pH_i sensitivities of G_c and apical, Ba^{2+}-sensitive NH_4^+ influx in IP-MTAL were virtually identical. The pH_i sensitivity of the Ba^{2+}-sensitive NH_4^+ influx in S-MTAL when exposed to (apical + basolateral) NH_4Cl was greater than that observed in IP-MTAL where NH_4Cl was added only to apical membranes, suggesting an additional effect of intracellular NH_4^+/NH_3 on NH_4^+ influx. NH_4^+ entry via apical $Na^+:K^+(NH_4^+):2Cl^-$ cotransport in IP-MTAL was somewhat more sensitive to reductions in pH_i than the Ba^{2+}-sensitive NH_4^+ influx pathway; NH_4^+ entry decreased by 52.9 ± 13.4% on reducing pH_i from 7.31 ± 0.17 to 6.82 ± 0.14. These results suggest that pH_i may provide a negative feedback signal for regulating

Address reprint requests to Dr. Steven C. Hebert, Renal Division, Department of Medicine, Brigham & Women's Hospital, 75 Francis St., Boston, MA 02115.

J. GEN. PHYSIOL. © The Rockefeller University Press · 0022-1295/92/03/0435/27 $2.00 435
Volume 99 March 1992 435–461

the rate of apical NH_4^+ entry, and hence transcellular NH_4^+ transport, in the MTAL. A model incorporating these results is proposed which illustrates the role of both pH_i and basolateral/intracellular NH_4^+/NH_3 in regulating the rate of transcellular N H_4^+ transport in the MTAL.

INTRODUCTION

The regulated excretion of NH_4^+ by the kidney is required for maintenance of systemic acid/base balance. NH_4^+ is synthesized in renal proximal tubule cells (Good and Burg, 1984) and preferentially secreted into the lumen of this nephron segment (Nagami and Kurokawa, 1985). Further downstream along the nephron, the thick ascending limb of Henle (TAL) actively reabsorbs NH_4^+ (Good and Burg, 1984; Good, Knepper, and Burg, 1984; Knepper, Packer, and Good, 1989). It has been proposed that NH_4^+ reabsorption by the TAL plays a major role in the maintenance of a high medullary interstitial concentration of NH_4^+, which in turn permits regulation of N H_4^+ excretion independently of H_2O excretion by the terminal portion of the nephron (Knepper et al., 1989).

Good et al. (1984) have shown that NH_4^+ absorption in the isolated perfused TAL occurs in the absence of a favorable transepithelial pH gradient, indicating that transepithelial pH trapping of NH_3 as NH_4^+ is not responsible for NH_4^+ reabsorption in the TAL. We have recently described the cellular mechanisms by which the mouse medullary segment of the TAL (MTAL) mediates active, transepithelial, pH-independent, transcellular NH_4^+ transport under isotonic conditions (Kikeri, Sun, Zeidel, and Hebert, 1989). These studies demonstrated that mouse MTAL cells are polarized such that apical membranes are virtually impermeable to NH_3 but highly permeable to NH_4^+, while basolateral membranes are highly permeable to NH_3 (Kikeri et al., 1989). NH_4^+ enters mouse MTAL cells from the lumen via both an apical Ba^{2+}-sensitive pathway (possibly an apical K^+ channel) and apical furosemide/bumetanide-sensitive $Na^+:K^+:2Cl^-$ cotransport (Kikeri et al., 1989). NH_4^+ appears to be carried on the K^+ site of the $Na^+:K^+:2Cl^-$ cotransporter in the TAL ($Na^+:K^+[NH_4^+]:2Cl^-$ cotransport [Kinne, Kinne-Saffran, Schuetz, and Schloelermann, 1986]). NH_4^+ exit from mouse MTAL cells occurs by H^+ extrusion via apical $Na^+:H^+$ exchange coupled to diffusion of NH_3 across basolateral membranes (Kikeri et al., 1989). The lumen-positive transepithelial voltage in the mouse MTAL, which is due to NaCl absorption (Hebert and Andreoli, 1984), may provide the driving force for the transport of protons from the lumen to the basolateral (interstitial) medium via the cation-selective paracellular pathway (Kikeri et al., 1989).

Because of the unusually high NH_4^+ permeability of apical membranes of MTAL cells, exposure to either apical or apical plus basolateral NH_4Cl results in a large cell acidification (Kikeri et al., 1989). Thus, NH_4^+ absorption by the MTAL is associated with potentially lethal reductions in pH_i. Some of the possible factors that could limit the magnitude of the NH_4^+-induced acidification of TAL cells include (*a*) the cellular buffering power, (*b*) acid extrusion via $Na^+:H^+$ exchange (Kikeri, Azar, Sun, Zeidel, and Hebert, 1990*a*) and possibly via an H^+-ATPase (Brown, Hirsch, and Gluck, 1988; Kikeri et al., 1990*a*), and (*c*) feedback inhibition of NH_4^+ entry pathways by either the NH_4^+-induced cell acidification or by intracellular NH_4^+/NH_3 itself (Oberleithner, Munich, Schwab, and Dietl, 1986; Paris and Pouyssegur, 1986). This latter possibility

was suggested by our earlier observation that the apical NH_4^+ entry pathways in the mouse MTAL (i.e., K^+ channels and Na^+:K^+:$2Cl^-$ cotransporters) did not appear to mediate significant exit of NH_4^+ from acidified cells (Kikeri et al., 1989).

The purpose of this study was to evaluate whether some or all of the aforementioned factors contribute to modulating the effects of NH_4^+ transport on pH_i in the mouse MTAL. Specifically, we used both the isolated perfused MTAL tubule and suspensions of MTAL tubules/cells from CD1 mice to determine the magnitude of the intracellular buffering power of MTAL cells and to assess the effects of pH_i on NH_4^+ entry into MTAL cells via the Ba^{2+}-sensitive NH_4^+ transport pathway and Na^+:K^+(NH_4^+):$2Cl^-$ cotransporter. Intracellular pH transients due to NH_4^+ entry into MTAL cells were measured using 2,7-biscarboxyethyl-5(6)-carboxyfluorescein (BCECF) and rates of NH_4^+-dependent H^+ flux calculated using the intrinsic cellular buffer power. The results of these studies support the view that both pH_i and basolateral/intracellular NH_4^+/NH_3 play an important role in regulating the rates of cellular NH_4^+ entry via the Ba^{2+}-sensitive pathway and Na^+:K^+(NH_4^+):$2Cl^-$ cotransport in MTAL cells. In addition, we have incorporated these results into a model that illustrates the role of both pH_i and NH_4^+/NH_3 in regulating NH_4^+ absorption by the MTAL.

METHODS

Cell Preparations

Two MTAL cell preparations from CD1 mice were used: suspensions of MTAL tubules (S-MTAL) and the isolated perfused MTAL (IP-MTAL).

S-MTAL were prepared as described previously (Kikeri et al., 1990*a*). Briefly, the inner stripe of the outer medulla from the kidneys of three to six mice were isolated and subjected to collagenase digestion; thereafter, MTAL tubules were separated from other tubule fragments by sedimentation through 3 g/dl albumin. The vast majority of tubules in these suspensions (>97%) were (*a*) morphologically identical to MTAL tubules in vivo, and (*b*) labeled with anti–Tamm Horsfall antibody, indicating that these suspensions consisted almost purely of MTAL tubules (Kikeri et al., 1990*a*). MTAL tubules in suspensions were functionally intact since they exhibited high rates of ouabain-sensitive (transport-related) oxygen consumption that was inhibited by either furosemide or bumetanide, and responded to arginine vasopressin by accumulating cyclic AMP (Kikeri et al., 1990*a*). In addition, these tubules had open lumens, allowing access of drugs/ions/inhibitors to apical membranes (Kikeri et al., 1990*a*). The advantages of using S-MTAL preparations include ease of preparation and the ability to obtain a large number of paired measurements in a single preparation. We have shown previously that transport data obtained in S-MTAL preparations were virtually identical to those obtained in IP-MTAL tubules (Kikeri et al., 1989, 1990*a*).

In experiments using IP-MTAL, tubules were isolated from the inner stripe of the outer medulla and perfused in vitro using methods previously described in detail (Hebert, Culpepper, and Andreoli, 1981*a*; Hebert and Andreoli, 1984, 1986). The perfused MTAL segments were 0.2–0.3 mm in length. Use of the IP-MTAL permitted evaluation of the sidedness (i.e., polarity) of transport processes.

Measurement of pH_i

Intracellular pH (pH_i) was measured in S-MTAL or IP-MTAL with BCECF using methods described by us previously (Kikeri et al., 1989, 1990*a*). BCECF-loaded MTAL tubules (S-MTAL

and IP-MTAL) exhibited uniform fluorescence at both 495 and 440 nm. Background fluorescence intensities (including cellular autofluorescence) were typically <1–2% of the total fluorescence after loading with BCECF.

S-MTAL. Tubule suspensions were transiently exposed (15 min at 25°C) to 2.5 μM of the tetra-acetoxymethyl ester of BCECF (BCECF-AM) and then washed free of extracellular dye. Fluorescence was monitored at 37°C in a computer-controlled SLM-Aminco SPF-500C spectrofluorometer (SLM Instruments, Inc., Urbana, IL) equipped with a water-jacketed, temperature-controlled cuvette holder and magnetic stirrer. A 50–75-μl aliquot of BCECF-loaded S-MTAL was diluted into a plastic cuvette containing 3 ml of medium and fluorescence was monitored at 530 nm emission wavelength, while the excitation wavelength rapidly alternated between 500 and 440 nm. After each experiment, the cells were pelleted in a microcentrifuge and the fluorescence of the extracellular medium was measured at both 500 and 440 nm. By subtracting the extracellular fluorescence intensities at 500- and 440-nm excitation wavelengths from the respective total fluorescence intensities obtained during the preceding experiment (due to intracellular + extracellular dye), fluorescence intensities due to intracellular dye were obtained (Kikeri et al., 1990*a*). We have previously shown that leakage of BCECF from S-MTAL occurs at very low rates (Kikeri et al., 1990*a*). The high K^+ (110 mM)/nigericin (5 μM) method of Thomas, Buchsbaum, Zimniak, and Racker (1979) was used to convert intracellular 500 nm/440 nm excitation ratios to units of pH_i over a pH_i range of 6.3–8 as described previously in detail by us (Kikeri et al., 1990*a*). Experiments were performed at 37°C in CO_2/HCO_3^--free medium containing (mM): 140 Na^+, 5 K^+, 148 mM Cl^-, 1 Ca^{2+}, 1 Mg^{2+}, 1 PO_4^{3-}, 20 mannitol, 10 glucose, 10 HEPES, and 0.2 g/dl albumin, equilibrated with 100% O_2, pH 7.4.

IP-MTAL. Standard CO_2/HCO_3^--free perfusing and bathing media contained (mM): 140 Na^+, 5 K^+, 149.4 Cl^-, 1 Ca^{2+}, 1.2 Mg^{2+}, 3 HEPES, 5 L-alanine, and 5.5 glucose, equilibrated with 100% O_2, pH 7.4, at 37°C. Bathing media also contained 0.2 g/dl Fraction V BSA. NH_4Cl, when added, replaced an equimolar amount of NaCl so that total osmolality and ionic strength remained constant. The perfusion flow rate was maintained between 10 and 20 nl/min, which is sufficient to minimize axial changes in perfusate ion concentrations and to chemically clamp the spontaneous transepithelial voltage along the length of the tubule. The flow rate of the bathing medium was maintained at 10–15 ml/min, which is sufficient to change completely the bath solution in <5 s (Hebert, Culpepper, and Andreoli, 1981*b*). Tubules were loaded with BCECF by transient exposure (10 min) to 10 μM BCECF-AM in the bathing medium. Fluorescence was alternately measured at excitation wavelengths of 495 and 440 nm (emission wavelength = 530 nm) using a computer-controlled inverted fluorescence microscope system (Carl Zeiss, Inc., Thornwood, NY) (Boyarsky, Ganz, Sterzel, and Boron, 1988; Kikeri et al., 1989, 1990*a*). Background fluorescence was subtracted from fluorescence intensity at each excitation wavelength to obtain intensities of intracellular fluorescence.

Calibration runs relating 495 nm/440 nm excitation ratio and pH_i (over a pH_i range of 6.2–7.7) were performed in three perfused tubules using medium containing 110 mM K^+ and 5 μM nigericin (medium pH 6.2–7.7). Fluorescence ratios at the various pH_i levels in the calibration runs were normalized such that the 495 nm/440 nm ratio at a pH_i of 7.2 was arbitrarily set at a value of 1. Fig. 1 shows a computer-fitted pH titration curve relating the normalized 495 nm/440 nm excitation ratios and pH_i as described initially by Boyarski et al. (1988). To convert fluorescence ratios obtained during an experiment on an individual IP-MTAL, the pH_i was set at 7.2 by exposure to 110 mM K^+/5 μM nigericin (medium pH 7.2) at the end of the given experiment, and the 495 nm/440 nm ratio was then measured (single point calibration). Fluorescence ratios obtained during the experimental period were normalized such that the 495 nm/440 nm ratio obtained with the single point calibration was equal to one, and then the fitted titration curve shown in Fig. 1 was used to convert the normalized experimental ratios to units of pH_i (Boyarsky et al., 1988).

To compare initial rates of pH_i change ($d(pH_i)/dt$) in either S-MTAL or IP-MTAL, the apparent initial rate of pH_i change was obtained either by measuring the slope of a computer-fitted linear regression over the initial ~5 s of pH_i change, or by measuring the tangent at the initial time point of an exponential curve computer-fitted to the initial time course of pH_i change. These transformations require no assumptions as to the mechanisms of pH_i change. Correlation coefficients for these fitted curves averaged 0.96 ± 0.02.

The initial rate of acid/base flux (J_H^+, millimolar per minute) at a given pH_i ($(pH_i)_x$) was calculated using measurements of $d(pH_i)/dt$ (in pH_i units per minute) at $(pH_i)_x$ and total buffering power (β_t, millimolar per pH_i) at $(pH_i)_x$ (Fig. 3) as (Boyarsky et al., 1988):

$$J_H^+ = \left[\left(\frac{dpH_i}{dt}\right)_{at(pH_i)_x}\right] \times (\beta_t)_{at(pH_i)_x} \quad (1)$$

These "flux" values in millimolar per minute can be converted to standard units (picomoles per second per square centimeter; see footnote 2) by using an MTAL tubule of 20 μm i.d. and a

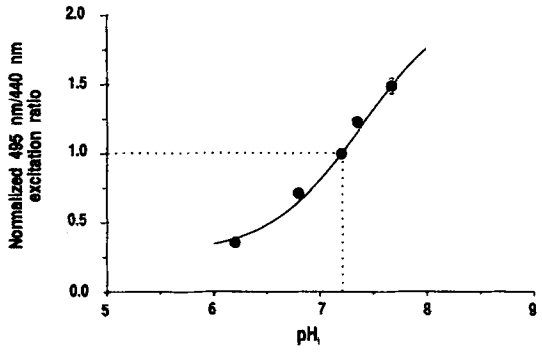

FIGURE 1. Calibration of BCECF fluorescence in IP-MTAL (n = 3). pH_i was set at varying levels using the high K^+/nigericin technique (Thomas et al., 1979) and 495 nm/440 nm excitation ratios were obtained. The 495 nm/440 nm excitation ratios have been normalized so that the ratio was 1 at a pH_i of 7.20. The curve shows a computer-fitted pH titration curve (r = 0.98; Boyarsky et al., 1988).

tubule cell volume of 0.25 nl/mm (Hebert, 1986). Comparisons among flux values reported in this paper and expressed in millimolar per minute assume that the surface-to-volume ratio for the tubule remains constant or changes negligibly.

Electrical Measurements in IP-MTAL

The electrical system used for the measurement of transepithelial voltage (V_e; millivolts) and transepithelial conductance (G_e; millisiemens per square centimeter) was identical to that used previously in this laboratory (Hebert et al. 1981*a*, *b* ; Hebert and Andreoli, 1984, 1986). Briefly, the perfusion pipette was made from 2 mm o.d. theta-style electrode glass (Hilgenberg, Malsfeld, Germany) that was divided axially by a septum, permitting virtually complete electrical separation of perfusion and current passing circuits. The perfusion half of the pipette also served as an electrical bridge for measurement of V_e (lumen with respect to bath). Electrical connections were made to the free flowing perfusate and bath with 3 M KCl/Ag/AgCl bridges (MERE-2; World Precision Instruments, Sarasota, FL). V_e at the collecting end of the perfused tubule was measured with a Ag/AgCl wire placed into the collecting fluid and connected to a high impedance electrometer (VF-2; World Precision Instruments). Biphasic direct current pulses (I_o [nanoamperes]; range = ±600; duration ≃ 1 s) were generated by a computer-linked voltage–current clamp (VCC 600; Physiological Instruments, San Diego, CA). The magnitudes of I_o, V_e, and voltage changes associated with current pulses were digitized (DT 2801; Data

Translation, Marlboro, MA) and stored on an IBM PC-XT computer. Transepithelial conductance (G_e) was calculated using terminated cable equations as described previously (Hebert et al., 1981*b*; Hebert and Andreoli, 1986).

Measurement of transcellular conductance (G_c). In the absence of NH_4^+ apical membranes of the mouse MTAL are predominantly, if not exclusively, conductive to potassium via K^+ channels (Hebert and Andreoli, 1984; Hebert, Friedman, and Andreoli, 1984). Recent patch clamp studies have demonstrated that this K^+ channel is inhibited by Ba^{2+} (Bleich, Schlatter, and Greger, 1990; Wang, White, Geibel, and Giebisch, 1990), and we have previously shown that the apical K^+ conductive pathway in mouse IP-MTAL can be completely blocked by the addition of 20 mM luminal Ba^{2+} in the absence of luminal K^+ (Hebert and Andreoli, 1986). Thus, the magnitude of G_e observed in the presence of 20 mM Ba^{2+}/0 K^+ in the luminal medium provides an estimate of the transepithelial shunt (paracellular) conductance (G_s), and the difference between G_e observed with 0 mM Ba^{2+}/5 mM K^+ vs. 20 mM Ba^{2+}/0 mM K^+ ($G_e^{20\,Ba/0\,K}$) provides a good approximation of G_c, the transcellular conductance (Hebert and Andreoli, 1986).

$$G_e = G_c + G_s \tag{2a}$$

$$G_s = G_e^{20Ba/0K} \tag{2b}$$

$$G_c = G_e - G_e^{20Ba/0K} \tag{2c}$$

The luminal Ba^{2+}-sensitive G_e (or G_c) in the IP-MTAL was used to indirectly assess the activity of apical K^+ channels. This method was used because of the difficulty in obtaining adequate long-term microelectrode impalements required for the experimental protocols used. Changes in G_c have been used previously by us to estimate changes in apical and basolateral conductive pathways (Hebert and Andreoli, 1986; Molony and Andreoli, 1988). In this study, all the electrical experiments were performed in the presence of arginine vasopressin (AVP; 10 μU/ml; $\sim 5 \times 10^{-11}$ M) in the bathing medium. This concentration of AVP produces a maximal increase in G_c without affecting G_s (Hebert and Andreoli, 1984). The AVP-induced increase in apical G_c allowed us to detect small degrees of inhibition in G_c. Standard CO_2/HCO_3^--free perfusing and bathing media used in the electrical experiments were identical to those used in the pH_i experiments.

Drugs and Reagents

BCECF-AM was obtained from Molecular Probes, Inc. (Eugene, OR). All other agents were obtained from Sigma Chemical Co. (St. Louis, MO), and were of analytical grade.

Statistics

Results on a single S-MTAL preparation or IP-MTAL constituted a single *n*. Unless stated, each experimental maneuver was repeated on at least three separate S-MTAL preparations or IP-MTALs. All experimental results are expressed as means ± SE. The Student's *t* test was used to analyze paired data, while ANOVA was used to evaluate unpaired groups; $P < 0.05$ was considered significant.

RESULTS

Cellular Buffering Power

Fig. 2 shows a plot of the intrinsic buffering power (β_i; millimolar per pH_i unit) of mouse MTAL cells over the pH_i range 6.5–7.6. β_i was measured in S-MTAL as (Roos

and Boron, 1981; Boyarsky et al., 1988):

$$\beta_i = -\frac{\Delta A}{\Delta pH} \tag{3}$$

where ΔA is the millimolar amount of acid added and ΔpH is the resultant drop in pH. The initial intracellular pH (segment a-b) was varied by altering extracellular pH (pH_o) from 6.4 to 7.9. Known intracellular proton loads were then acutely delivered to MTAL cells at point b by either the abrupt removal of extracellular NH_4Cl (5 mM, pK = 9) or the abrupt addition of extracellular sodium acetate (10 mM, pK = 4.75), and the acute drops in pH_i (segment b-c) were monitored (Roos and Boron, 1981; Zeidel, Silva, and Seifter, 1986; Boyarsky et al., 1988). The acetate addition protocol was used to deliver acute proton loads (Zeidel et al., 1986) at pH_i levels > 7.1, since the pH_i of S-MTAL in NH_4^+-containing medium was <7.1. To prevent pH_i regulation by $Na^+:H^+$ exchangers and HCO_3^- transporters (Kikeri et al., 1990*a*), experiments were performed in CO_2/HCO_3^--free and Na^+-free medium containing amiloride

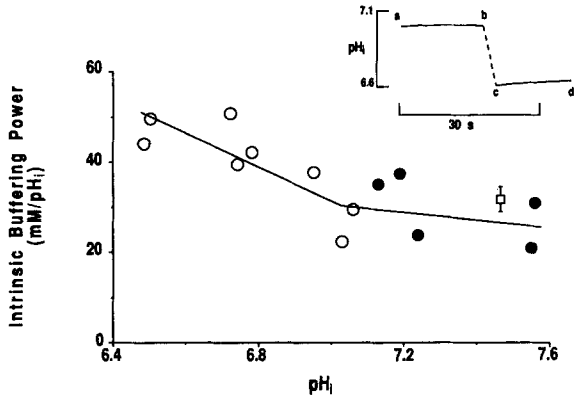

FIGURE 2. Intrinsic buffering power of MTAL cells. *Open circles,* NH_4Cl withdrawal; *solid circles,* sodium acetate addition; *open square,* addition of NH_4Cl in the presence of 10 mM Ba^{2+}, 1 mM furosemide, and 5 mM ouabain (see text for details). (*Insert*) Effect of NH_4Cl withdrawal. Experiments were performed in the absence of extracellular Na^+ (Na^+ replaced with *N*-methyl-D-glucamine$^+$) in the presence of 0.1–0.5 mM amiloride. Segment a-b represents pH_i in medium containing 5 mM NH_4Cl, pH_o 7.44. At b, extracellular NH_4Cl was abruptly withdrawn.

(0.1–0.5 mM). In addition, we assumed that $[NH_3]_i = [NH_3]_o$ and $[\text{acetic acid}]_i = [\text{acetic acid}]_o$ in the presence of extracellular NH_4^+ and acetate, respectively. The very slow rate of pH_i recovery after either extracellular NH_4^+ removal or extracellular acetate addition (Fig. 2, *insert,* segment c-d) indicated that acid extrusion or acetate$^-$ entry was negligible in the absence of extracellular Na^+.

It is evident from Fig. 2 that the intrinsic buffering power remained relatively stable over a pH_i range of 7.0–7.6 (β_i = 29.7 ± 2.4 mM/pH_i at a pH_i of 7.22 ± 0.08, n = 8; slope not significantly different from zero), but gradually increased with cell acidification below a pH_i of 7.0 ($\beta_i \approx$ 50 mM/pH_i at pH_i 6.5). An inverse relationship between β_i and pH_i has been previously described in other cell types by us (Kikeri, Zeidel, Ballermann, Brenner, and Hebert, 1990*b*) and others (Roos and Boron, 1981; Boyarsky et al., 1988). In addition, the observed values for β_i in MTAL cells are similar to those reported for proximal tubule cells (43 mM/pH_i [Krapf, Alpern, Rector, and Berry, 1987]) and white blood cells (28 mM/pH_i [Grinstein and Furuya,

1986]), but are approximately three- to sixfold greater than those reported for smooth muscle cells (9 mM/pH_i in A10 cells at pH_i 7.2 [Kikeri et al., 1990*b*]; 9 mM/pH_i at pH_i ~7.0 [Aickin, 1984]) or glomerular mesangial cells (5 mM/pH_i at pH_i 7.3 [Boyarsky et al., 1988]).

In additional experiments ($n = 5$) we estimated β_i at pH_i levels >7.1 pH units by adding 5 mM NH_4Cl to S-MTAL (in standard Na^+-containing, CO_2/HCO_3^--free medium, pH_o 7.4) in the presence of inhibited cellular NH_4^+ transport (i.e., in the presence of the combination of 10 mM barium, 1 mM furosemide, and 5 mM ouabain [Kikeri et al., 1989]), and measuring the acute increase in pH_i (pH_i 0.16 ± 0.02; see upper tracings of Figs. 4 and 9). Values of B_i obtained under these conditions (30.9 ± 3.0 mM/pH_i at a mean pH_i over the acute pH_i of 7.48 ± 0.01, $n = 5$; Fig. 2, open square) were similar to those obtained using acetate addition or NH_4^+ withdrawal at pH_i levels >7.0.

Cellular NH_4^+ Entry Pathways in Mouse MTAL

Addition of NH_4^+ to the luminal perfusate in the IP-MTAL leads to a prompt cell acidification due to NH_4^+ influx across the NH_3-impermeable apical membrane, and this NH_4^+-mediated fall in pH_i can be abolished by prior exposure of the apical membrane to the combination of luminal 0.1 mM furosemide and 10–20 mM luminal Ba^{2+} (Kikeri et al., 1989). In these experiments we assessed the relative contribution of each of these two pathways to NH_4^+ entry across apical membranes of the IP-MTAL. Rates of cell acidification due to luminal addition of 0.1 mM NH_4^+ were measured before and 3–5 min after addition of either 0.1 mM furosemide or 10 mM Ba^{2+} to luminal perfusate. Under these conditions, which mimic concentrations of NH_4^+ observed in vivo, $[NH_4^+]_i$ would be negligible due to the high NH_3 permeability of the basolateral membrane and the absence of basolateral medium NH_4Cl. Consequently, we assumed that $B_t = B_i$. Moreover, since acid extrusion (predominantly via apical Na^+:H^+ exchange [Kikeri et al., 1990*a*]) and acid loading are equal at the steady-state pH_i, the initial rate of H^+ influx (calculated according to Eq. 1) on addition of luminal NH_4Cl reflects the initial rate of cellular NH_4^+ influx.[1] In four IP-MTAL tubules, addition of 0.1 mM NH_4Cl to K^+-free luminal medium at the steady-state pH_i (7.38 ± 0.11, $n = 4$) resulted in an initial NH_4^+ influx rate of 21.7 ± 3.3 mM/min and this NH_4^+ influx was completely blocked by addition of both 0.1 mM furosemide and 10 mM Ba^{2+} to the luminal medium. 0.1 mM apical furosemide inhibited apical NH_4^+ entry by 55.3 ± 6.1% (11.7 ± 1.9 mM/min) and 10 mM apical Ba^{2+} inhibited apical NH_4^+ entry by 44.8 ± 6.1% (10 ± 2.9 mM/min). Thus in the absence of inhibitors, both the apical Ba^{2+}-sensitive pathway and Na^+:K^+(NH_4^+):$2Cl^-$ cotransporter mediated significant apical entry of NH_4^+ into mouse MTAL cells at ammonium concentrations observed in vivo.

Fig. 3 shows the initial rate of apical NH_4^+ entry in IP-MTAL, via both the Ba^{2+}- and furosemide-sensitive pathways, after addition of NH_4Cl to luminal fluid at concentrations from 0.1 to 20 mM ($n = 8$ tubules). Steady-state pH_i in NH_4^+-free medium

[1] This was substantiated by our previous observation that that removal of luminal NH_4Cl (in the absence of basolateral NH_4Cl) results only in a small cell acidification even in the absence of pH_i regulation (Kikeri et al., 1989).

averaged 7.26 ± 0.04 pH units. In these experiments, media contained 100 mM Na^+ and 40 mM *N*-methyl-D-glucamine$^+$ ($NMDG^+$); NH_4^+ replaced $NMDG^+$ in an equimolar manner. The apparent $K_{0.5}$ and the maximal rate of luminal NH_4^+ entry were 0.5 and 83.3 mM/min, respectively.[2] This low $K_{0.5}$ value may be due both to the high affinity of NH_4^+ for the Na^+:K^+(NH_4^+):2Cl^- cotransporter (Kinne et al., 1986) and to inhibition of both apical NH_4^+ entry mechanisms by factors such as pH_i (this possibility is evaluated in the experiments described below).

To determine if NH_4^+ could enter MTAL cells via the basolateral Na^+:K^+-ATPase, ouabain-sensitive acidification was evaluated in S-MTAL in the presence of 0.5–20 mM NH_4Cl (n = 5). Steady-state pH_i of S-MTAL in NH_4^+-free medium averaged

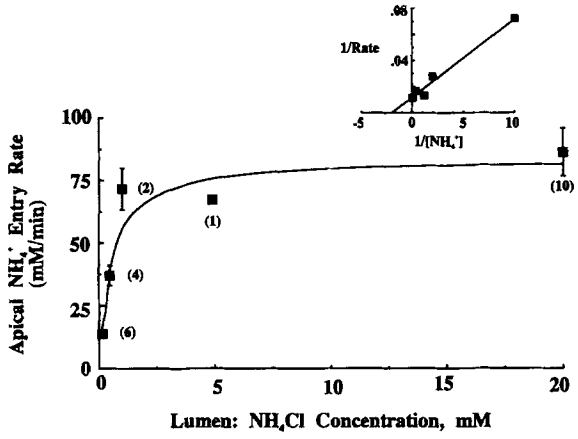

FIGURE 3. Effect of luminal medium NH_4Cl concentration on the initial rate of apical, NH_4Cl-dependent H^+ influx (NH_4^+ entry) in IP-MTAL. NH_4Cl was acutely added to the luminal medium in IP-MTAL and the initial rate of acidification was measured. The number in parentheses next to each symbol indicates the number of measurements. The curve represents the least-squares fit of the Michaelis-Menten relationship to the data (r = 0.99). The inset plot shows the double-reciprocal plot of the data (r = 0.99; 1/rate = 0.006(1/[NH_4^+]) + 0.012; $K_{0.5}$ = 0.5 mM; maximal rate of influx = 83.3 mM/min).

7.42 ± 0.02 pH units (n = 16). In the experiments shown in Fig. 4, which were performed on a representative S-MTAL preparation, segments a-b represent steady-state pH_i of S-MTAL in NH_4^+-free medium, pH_o 7.4. 5 mM NH_4Cl was then added to the extracellular medium at point b. The lower trace shows the control acidification response after addition of 5 mM NH_4Cl to the medium bathing apical and basolateral membranes of S-MTAL (b-g). However, addition of 5 mM NH_4Cl in the presence of 10 mM Ba^{2+}, 1 mM furosemide, and 5 mM ouabain resulted in rapid cell alkalinization due to entry of NH_3 across NH_3-permeable basolateral membranes (Kikeri et al., 1989; compare c-d with b-g). Thus, the combination of Ba^{2+}, furosemide, and ouabain inhibited virtually all the entry of NH_4^+ into MTAL cells. The pH_i on addition of NH_4Cl in the presence of inhibited NH_4^+ transport was similar to the pH_i expected if cell membranes were permeable only to NH_3. In other words, inhibition of NH_4^+ transport by the combination of barium plus furosemide and ouabain converted the

[2] The maximal rate of luminal NH_4^+ entry of 83.3 mM/min can be converted to more conventional transport units, assuming a MTAL tubule inner diameter of 20 μm and a MTAL tubule cell volume of 0.25 nl/mm tubule length (Hebert, 1986). Using these parameters, ${}^{max}J_{NH_4}{}^+$ = 20 pmol/min·mm or 550 pmol/s·cm^2. These rates are consistent with rates of net NH_4^+ absorption observed in perfused thick ascending limb tubules (Knepper et al., 1989).

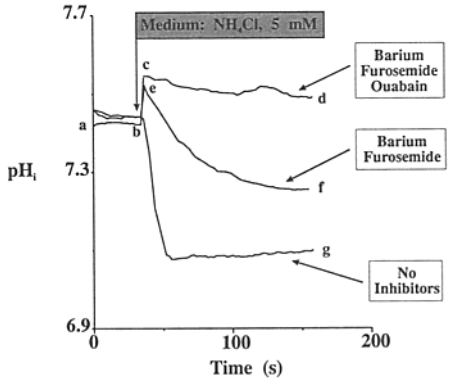

FIGURE 4. Role of Na^+:K^+-ATPase in mediating cellular NH_4^+ entry in S-MTAL. Segments a-b, resting pH_i. At b, 5 mM NH_4Cl was added to the extracellular medium either in the presence of 10 mM Ba^{2+}, 1 mM furosemide, and 5 mM ouabain (b-c-d), in the presence of 10 mM Ba^{2+} and 1 mM furosemide (b-e-f), or in the absence of inhibitors (b-g).

highly NH_4^+-permeable, native S-MTAL cells into almost purely NH_3-permeable cells (across basolateral membranes). The selective removal of ouabain resulted in partial restoration of the acidification response to 5 mM NH_4Cl addition (e-f). The ouabain-sensitive rate of NH_4^+ entry with 20 mM extracellular NH_4Cl was 17.4 ± 0.4 mM/min (calculated as initial rates [e-f] − [c-d]; n = 3). In separate experiments performed in the absence of NH_4Cl, the addition of either the combination of Ba^{2+}, furosemide, and ouabain or the combination of Ba^{2+} and furosemide to S-MTAL did not alter steady-state pH_i over 200 s (ΔpH_i = 0.01 ± 0.02, n = 2). Thus, the basolateral, ouabain-sensitive Na^+:K^+-ATPase could mediate NH_4^+ entry into MTAL cells.

Effect of pH_i on Total Rate of NH_4^+ Entry via Ba^{2+}-, Furosemide-, and Ouabain-sensitive Pathways in S-MTAL

Fig. 5 illustrates the effect of pH_i on the total rate of cellular NH_4^+ entry in a representative S-MTAL preparation, i.e., via the combination of the Ba^{2+}-sensitive N H_4^+ transport pathway, the furosemide-sensitive Na^+:K^+(NH_4^+):$2Cl^-$ cotransporter,

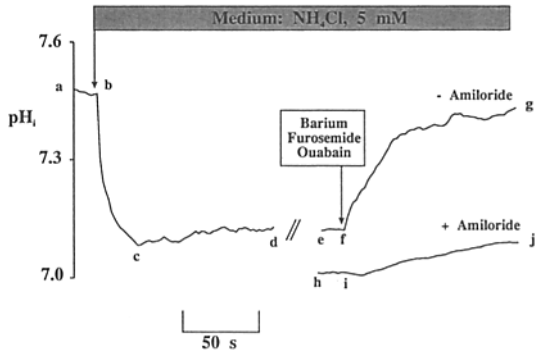

FIGURE 5. Effect of pH_i on the total rate of NH_4^+ entry into S-MTAL. Segment a-b, resting pH_i of S-MTAL in NH_4^+-free medium. At b, 5 mM NH_4Cl was added to the extracellular medium and was present for the duration of the experiment. The gap in the trace represents a 3.5-min incubation period after adding either 1 mM amiloride or vehicle (DMSO) to the extracellular medium at point d. At points f and i, 10 mM Ba^{2+}, 1 mM furosemide, and 5 mM ouabain were abruptly added.

and the ouabain-sensitive $Na^+:K^+(NH_4^+)$-ATPase. Segment a-b represents steady-state pH_i of S-MTAL in NH_4^+-free medium (7.45 ± 0.05, n = 3). Addition of 5 mM NH_4Cl at b reduced pH_i to a new steady-state level (7.13 ± 0.01, c-d). At d, either amiloride (1 mM) or vehicle (DMSO) was added to the medium. The gap in the trace represents a 2–4-min incubation period.

Abrupt inhibition of total NH_4^+ entry at point f, in the absence of amiloride, by adding the combination of 10 mM Ba^{2+}, 1 mM furosemide, and 5 mM ouabain resulted in rapid pH_i recovery (f-g). Since net rates of NH_4^+ entry (via the combination of Ba^{2+}-, furosemide-, and ouabain-sensitive pathways) and NH_4^+ exit (by proton extrusion via $Na^+:H^+$ exchange coupled with NH_3 diffusion across the basolateral membrane [Kikeri et al., 1989]) are probably equal during the steady state in N H_4^+-containing medium (e-f), the initial rate of acid extrusion at point f (initial pH_i recovery rate × β_t, where $\beta_t = \beta_i + \beta_{NH_3}$) of 33.7 ± 3.8 mM/min equals the total rate of ammonium entry (via the Ba^{2+}-, furosemide-, and ouabain-sensitive pathways) during segment e-f.

Amiloride addition in the presence of 5 mM ambient NH_4Cl at point d reduced pH_i within 1 min, because of inhibition of $Na^+:H^+$ exchange (Kikeri et al., 1990*a*), to a new steady-state level of 6.96 ± 0.02 (h-i). As discussed above, NH_4^+ entry and exit are equal during segment h-i. Inhibition of total NH_4^+ entry with the combination of Ba^{2+}, furosemide, and ouabain at point i led to a markedly reduced rate of acid extrusion (5.9 ± 0.07 mM/min). Since both apical and basolateral membranes of S-MTAL are exposed to NH_4Cl, and because basolateral membrane are highly permeable to NH_3, $[NH_4^+]_i$ would increase as pH_i decreases. Increases in $[NH_4^+]_i$, in turn, would reduce the chemical gradient favoring NH_4^+ uptake. Thus the combined effects of the reduction of pH_i from 7.13 ± 0.01 (e-f) to 6.96 ± 0.02 (h-i) and the associated rise in $[NH_4^+]_i$ reduced the total rate of cellular NH_4^+ entry across both apical and basolateral membranes by >80%.[3] In addition, these data indicate that $Na^+:H^+$ exchange plays the dominant role in NH_4^+ exit (H^+ extrusion coupled to NH_3 diffusion [Kikeri et al., 1989]) from mouse MTAL cells in the presence of ambient NH_4Cl.

Effect of pH_o/pH_i on Transcellular Conductance (G_c) in IP-MTAL

Because of the difficulty in obtaining long-term microelectrode impalements in the small epithelial cells of the mouse MTAL and the necessity of obtaining paired data (because of large tubule-to-tubule variations in transepithelial conductance [Hebert

[3] Amiloride does not appear to significantly affect any of the NH_4^+ entry processes. We (Kikeri et al., 1989) have shown that the combination of luminal 10 mM Ba^{2+} and luminal 0.1 mM furosemide completely abolishes the cell acidification observed with luminal 20 mM NH_4^+ addition in IP-MAL and that these two agents plus 5 mM ouabain completely block NH_4^+-induced cell acidification in S-MAL. In addition, in this paper (Fig. 3) we demonstrate that inhibition of the $Na^+:H^+$ exchanger (Na^+ replaced by $NMDG^+$) does not affect luminal NH_4^+-induced cell acidification in IP-MAL. Furthermore, we have previously shown (Fig. 4 in Kikeri et al., 1990*a*) that amiloride has no significant effect on QO_2, a sensitive index to the activity of both the apical $Na^+:K^+/NH_4^+:2Cl^-$ entry mechanism and the basolateral Na^+,K^+-ATPase exit mechanism. Finally, if amiloride had a significant effect on the K^+ channel then the cell would depolarize (for example, luminal Ba^{2+} depolarizes the mouse MTAL cell; Hebert and Andreoli, 1984) and the cell would be expected to alkalinize somewhat because the driving force for H^+ entry would be reduced.

and Andreoli, 1984, 1986]), we used an alternative approach to estimate the effects of pH_o/pH_i on the apical Ba^{2+}-sensitive K^+ conductance using measurements of transcellular conductance (G_c). As described in detail in Methods (see Eqs. 2a–2c), the difference between transepithelial conductance (G_e) measurements observed in IP-MTAL with perfusate containing either 0 mM Ba^{2+}/5 mM K^+ (total G_e) or 20 mM Ba^{2+}/0 mM K^+ (shunt conductance, G_s) provides a good approximation of the transcellular conductance, G_c. This approach has provided valuable information on the regulation of cellular conductive pathways in the MTAL in previous studies (Hebert and Andreoli, 1984, 1986; Molony and Andreoli, 1988).

G_e decreased from 110.9 ± 4.4 to 40.4 ± 1.2 mS/cm^2 ($n = 4$; $P < 0.01$) on changing the luminal medium from 0 mM Ba^{2+}/5 mM K^+ to 20 mM Ba^{2+}/0 mM K^+ at a constant luminal medium pH of 7.4, indicating that G_c and G_s accounted for

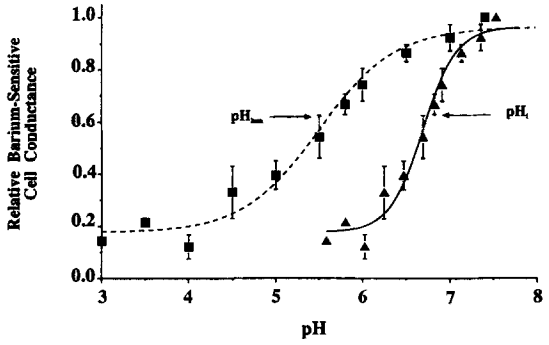

FIGURE 6. Effect of pH_{lum} and pH_i on relative Ba^{2+}-sensitive cell conductance (G_c) in IP-MTAL (see Methods and Eqs. 2a–2c for procedure for assessing G_c). The solid squares and dashed line show the relationship between pH_{lum} and relative G_c, while the solid triangles show the relationship between pH_i and relative G_c. The relation

$$\text{relative rate} = A + B \cdot \left[\frac{10^{(pH-pK)}}{1 + 10^{(pH-pK)}}\right]$$

where A and B are the intercept and slope, respectively, was fit to the data. pK = 6.7 ($r = 0.95$) for the pH_i fit.

approximately two-thirds and one-third of G_e, respectively. Similar G_s:G_e ratios were also observed in previous studies (Hebert and Andreoli, 1984, 1986). In another set of experiments ($n = 4$) the luminal medium pH (pH_{lum}) was reduced in a stepwise manner from pH 7.4 to pH 3.0 in the presence of luminal 0 mM Ba^{2+}/5 mM K^+. The solid squares in Fig. 6 show the relative changes in G_c, normalized such that G_c at pH_{lum} 7.4 was arbitrarily set at 1. Changing the luminal medium from 0 mM Ba^{2+}/5 mM K^+ to 20 mM Ba^{2+}/0 mM K^+ at a constant pH_{lum} of 4 did not alter G_e ($G_e^{0Ba} = 22.3 \pm 5.7$; $G_e^{20Ba} = 31.9 \pm 11.1$; $\Delta G_e = -9.6 \pm 5.4$, $n = 4$, NS). Therefore, reducing pH_{lum} from 7.4 to 4.0 abolished virtually all the cell conductance but had no significant effect on G_s. These data demonstrate indirectly that the apical Ba^{2+}-sensitive K^+ conductance was sensitive to luminal medium pH.

The experiments shown in Fig. 7 were performed to determine the effect of pH_{lum} on pH_i in the IP-MTAL (n = 4). Using experimental conditions identical to those used in the electrical experiments, pH_{lum} was reduced in a stepwise manner from pH 7.4 to pH 5.0 (luminal medium contained 0 mM Ba^{2+}/5 mM K^+) and pH_i was monitored at each luminal medium pH level. As shown in Fig. 7, pH_i was greater than luminal medium pH at acidic pH_i levels, possibly because of pH_i regulation by Na^+:H^+ exchange, while pH_i was less than luminal medium pH at medium pH levels > 7.5 pH units. This relationship between luminal medium pH and pH_i shown in Fig. 7 was then used to determine the relationship between pH_i and relative apical Ba^{2+}-sensitive transcellular conductance (solid triangles, Fig. 6). As shown in Fig. 6, the relative G_c was related, over a pH_i range of 6.0–7.4, to pH_i with 50% inhibition at a pH_i of ~6.7 and/or to luminal pH_o with a 50% inhibition at pH_o ~5.5.

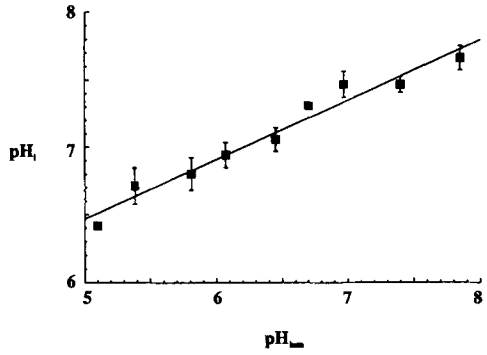

FIGURE 7. Effect of pH_{lum} on pH_i in IP-MTAL. The line is the least-squares fit of the data: $y = 0.442x + 4.26$, $r = 0.98$.

Effect of pH_i on NH_4^+ Entry due to Apical Ba^{2+}-sensitive NH_4^+ Transport in IP-MTAL

Since pH_i in the electrical experiments shown in Fig. 6 was altered by changing luminal medium pH, either luminal medium pH (pH_{lum}) or pH_i may have been responsible for the changes in G_c. Moreover, it is possible that the pH-dependent changes in G_c resulted from alterations in either apical or basolateral conductances, or both. We therefore assessed the effects of pH_i, independent of luminal pH_o changes, on NH_4^+ entry via the apical Ba^{2+}-sensitive NH_4^+ transport pathway in IP-MTAL (n = 5). The results of these experiments are shown in Fig. 8.

The rate of change in pH_i was measured after addition of 1 mM NH_4Cl to a luminal medium in which both Na^+ and K^+ were replaced isosmotically with $NMDG^+$ and to which 0.1 mM furosemide was added. Under these conditions the H^+ influx due to NH_4^+ entry represents exclusively the apical Ba^{2+}-sensitive NH_4^+ transport pathway. The initial rate of NH_4^+ influx, J_{NH_4} was then calculated according to Eq. 1. In addition, the removal of luminal Na^+ would abolish any H^+ efflux mediated by the apical Na^+:H^+ exchanger. For these experiments we also assumed that $\beta_t \approx \beta_i$ since intracellular NH_4^+/NH_3 concentrations would be low due to the absence of basolateral NH_4Cl and the high basolateral membrane NH_3 permeability (Kikeri et al., 1989).

To assess the effect of pH_i on the Ba^{2+}-sensitive (i.e., furosemide-insensitive) apical J_{NH_4} the pH_i (before luminal NH_4^+ addition) was altered by changing the pH of the

basolateral bath solution in stepwise fashion over the range 4–8. The relationship between basolateral pH_o and pH_i was virtually identical to that observed for apical pH_o and pH_i (Fig. 7). As shown in Fig. 8, the relative rate of furosemide-insensitive, apical NH_4^+ entry, normalized to the influx rate obtained at $pH_i \sim 7.3$, was dependent on pH_i in IP-MTAL tubules with reductions in pH_i inhibiting the apical NH_4^+ flux. At pH_i values < 6.5, J_{NH_4} was inhibited $> 80\%$ compared with J_{NH_4} values at $pH_i > 7.5$. In four additional IP-MTAL tubules, pH_i was reduced with luminal amiloride (0.5 mM) in the presence of luminal Na^+ and 0.1 mM furosemide (apical and basolateral pH_o 7.40; Fig. 8, open squares). Inhibition of apical Na^+:H^+ exchange resulted in a decrease in pH_i of $\sim 2.6 \pm 0.03$ pH units and a fall in relative J_{NH_4} of $15.3 \pm 3.5\%$ (Fig. 8, open squares), a value that was indistinguishable from the relative reduction observed when pH_i was decreased by changing basolateral pH_o. The results in Fig. 8

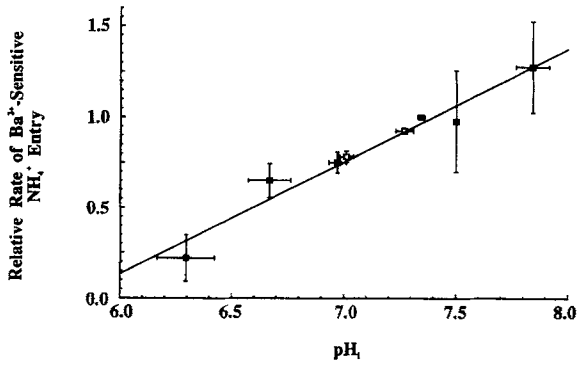

FIGURE 8. Effect of pH_i on the relative rate of NH_4^+ entry (millimolar per minute) via the apical Ba^{2+}-sensitive pathway in IP-MTAL. Experiments were performed in the absence of luminal Na^+ and K^+ and with 0.1 mM furosemide added to the luminal perfusate (n = 5 tubules; solid squares). NH_4^+ entry rates for each tubule were normalized to the entry rate observed at pH_i 7.3, which was set to 1.0. *Open squares,* experiments with and without luminal 0.5 mM amiloride (to inhibit the apical Na^+:H^+ antiporter) and in the presence of luminal Na^+ (n = 5). The solid line is a least-squares linear fit: $y = 16.23x - 106.16$ (r = 0.89).

demonstrate that reducing pH_i by variations in basolateral pH or by addition of luminal amiloride (at constant pH_o) inhibited NH_4^+ influx via the apical Ba^{2+}-sensitive NH_4^+ transport pathway. The observations in Figs. 6–8 that reductions in pH_i to similar values by decreasing luminal or basolateral pH_o or by luminal amiloride addition at a constant pH_o led to similar fractional reductions in Ba^{2+}-sensitive NH_4^+ entry (or K^+ conductance) suggests that cell pH rather than pH_o was the major factor affecting the Ba^{2+}-sensitive entry mechanism.

Effect of pH_i on NH_4^+ Entry due to Ba^{2+}-sensitive NH_4^+ Transport in S-MTAL

Determination of rate of NH_4^+ entry due to Ba^{2+}-sensitive NH_4^+ pathway. Fig. 9 shows in a representative experiment on a single S-MTAL preparation (*a*) the control acidification response on addition of 5 mM NH_4Cl at point b to S-MTAL (b-f), (*b*) the effect of 1 mM furosemide plus 5 mM ouabain on the acidification response (b-e), and (*c*) the effect of 10 mM Ba^{2+}, furosemide, and ouabain on the pH_i response to NH_4Cl addition (b-c-d). Addition of either furosemide plus ouabain or Ba^{2+}, furosemide plus ouabain in the absence of NH_4Cl did not alter steady-state pH_i (n = 2). As shown previously in Fig. 4 (upper curve), addition of extracellular NH_4Cl when NH_4^+

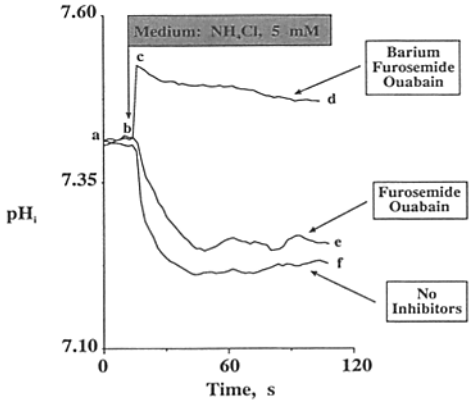

FIGURE 9. Ba^{2+}-sensitive NH_4^+ entry in S-MTAL. In this representative trace, segment a-b represents resting pH_i in NH_4^+-free medium. At b, 5 mM NH_4Cl was added in the presence of either the combination of 10 mM Ba^{2+}, 1 mM furosemide, and 5 mM ouabain (b-c-d) or the combination of furosemide and ouabain (b-e), or in the absence of inhibitors (b-f).

transport was completely inhibited (i.e., in the presence of the combination of Ba^{2+}, furosemide, and ouabain) resulted in virtually instantaneous (<2 s) alkalinization (b-c; $\Delta pH_i = 0.16 \pm 0.02$, $n = 5$). In either the presence of furosemide plus ouabain (middle curve) or the absence of inhibitors (lower curve), sustained, rapid acidification was observed. The initial rate of decrease in pH_i in the presence of furosemide plus ouabain was taken to represent the initial rate of NH_4^+ influx via Ba^{2+}-sensitive N H_4^+ transport pathways. J_{NH_4} was calculated according to Eq. 1, where $\beta_t = \beta_i + \beta_{NH_3}$. Since both apical and basolateral membranes in S-MTAL are exposed to ambient NH_4Cl, the observed J_{NH_4} values represent Ba^{2+}-sensitive NH_4^+ transport across both apical and basolateral membranes. Apical membranes of MTAL cells possess an apical Ba^{2+}-sensitive NH_4^+ transport pathway (Kikeri et al., 1989); whether a Ba^{2+}-sensitive NH_4^+ transport pathway exists on basolateral membranes of MTAL cells is unknown.

Effect of pH_i on NH_4^+ entry due to Ba^{2+}-sensitive NH_4^+ transport. The experiments shown in Fig. 10 were used to assess NH_4^+ entry via the Ba^{2+}-sensitive pathways in S-MTAL at various pH_i values using the strategy discussed above (Fig. 9). Addition of 5 mM NH_4Cl to the medium bathing S-MTAL at the resting pH_i resulted in a rapid

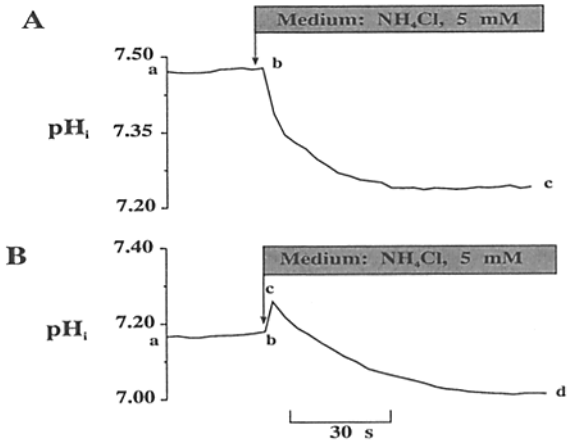

FIGURE 10. Effect of pH_i on Ba^{2+}-sensitive NH_4^+ entry in S-MTAL. These representative experiments were performed in the presence of 1 mM furosemide and 5 mM ouabain. (*A*) 5 mM NH_4Cl was added at the arrow. (*B*) Cells were preexposed to 0.5 mM amiloride for 2–4 min before starting the experiment, and 5 mM NH_4Cl was added at the arrow.

fall in pH_i (b-c). At a pH_i of 7.41 ± 0.02 (~2 s after addition of NH_4Cl; point b), the initial rate of Ba^{2+}-sensitive NH_4^+ entry in the presence of 5 mM NH_4Cl averaged 32.6 ± 3.1 mM/min (n = 7). Addition of amiloride to S-MTAL reduced pH_i from 7.43 ± 0.04 to 7.20 ± 0.03 within 1 min (n = 4, $P < 0.05$). The subsequent addition of 5 mM NH_4Cl to amiloride-treated cells (Fig. 10 *B*, point b) resulted in a small increase in pH_i to 7.26 ± 0.02 (segment b-c) followed by a much larger fall in pH_i (segment c-d). The small rise in pH_i with exposure to NH_4Cl suggests that the initial rate of H^+ entry due to Ba^{2+}-sensitive NH_4^+ transport at the acidic pH_i of 7.20 ± 0.03 was reduced relative to the rate of buffering of H^+ due to the rapid entry of NH_3 across the basolateral membrane. At a pH_i of 7.26 ± 0.02, the initial rate of Ba^{2+}-sensitive NH_4^+ entry averaged 18.8 ± 1.2 mM/min, a 42% reduction compared with the influx rate at pH_i 7.41 (n = 4).

Fig. 11 shows the direct relationship between pH_i and the initial rate of Ba^{2+}-sensitive NH_4^+ entry in S-MTAL. Decreases in Ba^{2+}-sensitive J_{NH_4} were observed both with the spontaneous variations in resting pH_i (open circles) and with the further reductions in pH_i resulting from exposure to amiloride (solid circles). When the

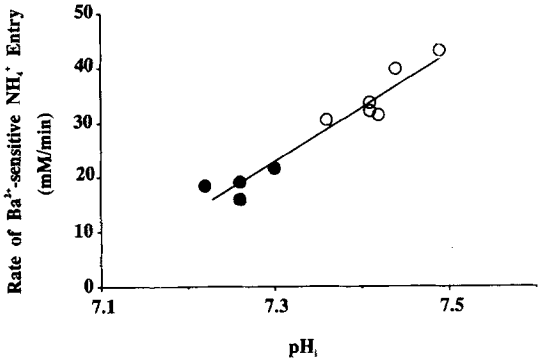

FIGURE 11. Relationship between initial pH_i and initial Ba^{2+}-sensitive H^+ influx (NH_4^+ influx) in the presence of 5 mM NH_4Cl in S-MTAL. *Closed circles*, entry rates in cells acidified by amiloride addition; *open circles*, untreated cells.

results in Fig. 11 are taken together with those in Figs. 8 and 6, it is clear that decreasing pH_i over the physiological range of 6.0–7.8 dramatically reduces the activity of the Ba^{2+}-sensitive K^+/NH_4^+ pathway in apical membranes.

Effect of pH_i on NH_4^+ Entry by Apical Na^+:K^+/NH_4^+:2Cl^- Cotransport in IP-MTAL

Experiments were performed in IP-MTAL to determine if NH_4^+ entry into MTAL cells via the apical Na^+:K^+(NH_4^+):2Cl^- cotransporter (Kinne et al., 1986; Kikeri et al., 1989) was sensitive to pH_i. Fig. 12 shows representative experiments in IP-MAL illustrating the effects of initial steady-state pH_i on the rate of acidification induced by addition of 20 mM NH_4Cl to K^+-free perfusate in the presence of 20 mM $BaCl_2$. Since the combination of furosemide (0.1 mM) and Ba^{2+} (10–20 mM) in the luminal medium inhibits all the apical NH_4^+ entry in IP-MTAL, the fall in pH_i observed on addition of luminal NH_4Cl in the presence of luminal Ba^{2+} represents NH_4^+ entry via the apical Na^+:K^+(NH_4^+):2Cl^- cotransporter. Luminal NH_4Cl was added at points a, c, e, and g. Segments a-b and c-d are the acidification responses in two tubules at the different spontaneous, initial, steady-state pH_i values a and c. Addition of 0.5 mM

amiloride to the luminal fluid in the absence of NH_4Cl resulted in acidification from a to e and from c to g in these two tubules: the average amiloride-induced drop in pH_i was 0.49 pH units ($n = 4$).[4] The data in Fig. 12 clearly demonstrate that as the initial steady-state pH_i is reduced, the rate of cellular acidification mediated by luminal NH_4^+ influx via the cotransporter is considerably slowed.

Fig. 13 shows the direct relationship between the initial steady-state pH_i and the initial rate of NH_4^+ entry via apical $Na^+:K^+(NH_4^+):2Cl^-$ cotransporter. Note that the open squares show the usual spontaneous variability of resting pH_i; in the absence of

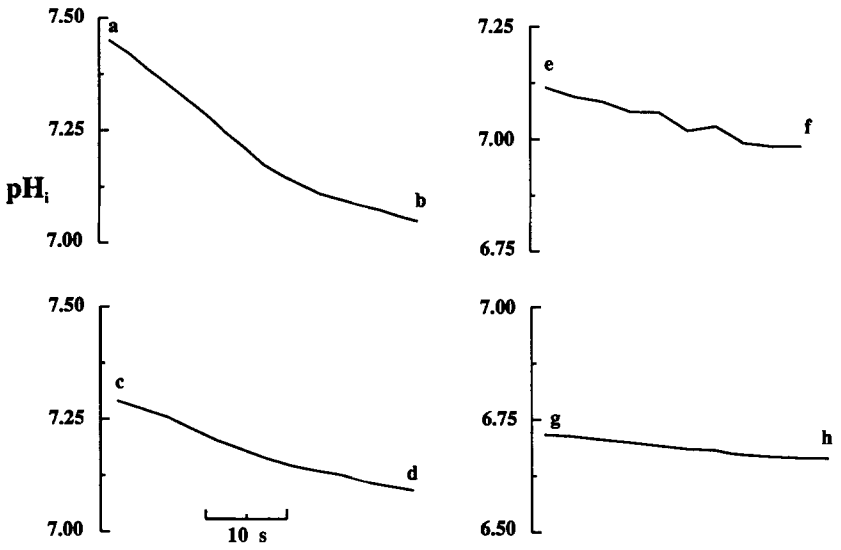

FIGURE 12. Effect of pH_i on NH_4^+ entry rate via apical $Na^+:K^+(NH_4^+):2Cl^-$ in IP-MTAL. Reducing pH_i by luminal addition of 0.5 mM amiloride (from 7.31 ± 0.17 to 6.82 ± 0.14; not shown in figure) decreased the initial rate of apical, furosemide-sensitive H^+ entry rate on addition of 0.1 mM NH_4Cl to the luminal medium by 52.9 ± 13.4%.

amiloride these spontaneous variations in pH_i correlated closely with the observed rate of ammonium entry. The amiloride-mediated reduction in pH_i from 7.31 ± 0.17 to 6.8 ± 0.14 pH units was associated with a 52.9 ± 13.4% decrease in the rate of N H_4^+ influx via the $Na^+:K^+(NH_4^+):2Cl^-$ cotransporter. Thus, apical NH_4^+ entry via the furosemide-sensitive cotransporter, like that through the Ba^{2+}-sensitive apical pathway, was markedly sensitive to pH_i.

[4] It should be noted that the decrease in pH_i in IP-MTAL with luminal amiloride addition in the presence of luminal Ba^{2+} (0.49 pH units) was larger than that observed in the presence of furosemide (0.26 pH units in IP-MTAL; 0.23 pH units in S-MTAL). Although the reason for this difference was not evaluated further in this study, it is possible that reduction of metabolic acid production because of inhibition of salt transport-related energy consumption by furosemide (in the MTAL, furosemide-sensitive oxygen consumption accounts for > 50% of the total rate of oxygen consumption [Kikeri et al., 1990*a*]) may partially explain this difference.

DISCUSSION

The results of this study demonstrate that (*a*) NH_4^+ is transported at high affinity and at high rates across apical membranes of MTAL cells via a Ba^{2+}-sensitive NH_4^+ transport pathway and Na^+:K^+(NH_4^+):$2Cl^-$ cotransport; (*b*) NH_4^+ entry via both the Ba^{2+}-sensitive NH_4^+ transport pathway and Na^+:K^+(NH_4^+):$2Cl^-$ cotransport was sensitive to pH_i over a pH_i range of 6.8–7.2 pH units; (*c*) the effect of pH_i on NH_4^+ entry via the Ba^{2+}-sensitive pathway was greater in S-MTAL (42% reduction on decreasing pH_i from 7.41 to 7.26) than in IP-MTAL (15% reduction on decreasing pH_i from 7.27 to 7.01), suggesting a modulatory effect of NH_3/NH_4^+; and (*d*) NH_4^+ could enter MTAL cells via the basolateral Na^+:K^+-ATPase, i.e. Na^+:K^+(NH_4^+)-ATPase.

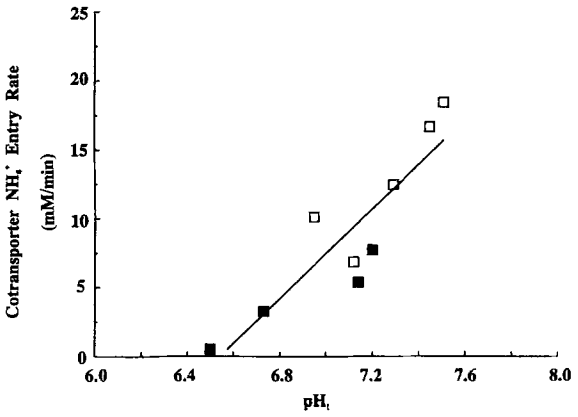

FIGURE 13. Relationship between pH_i and the rate of NH_4^+ entry via the apical Na^+:K^+(NH_4^+):$2Cl^-$ cotransporter in IP-MAL. pH_o 7.40 in all experiments. *Closed circles*, entry rates in tubule cells acidified by addition of 0.5 mM amiloride; *open circles*, untreated tubules. The curve is the least-squares linear fit ($y = 16.2x - 106.2$; $r = 0.86$).

NH_4^+ Transport by the Ba^{2+}-sensitive Pathway and Na^+:K^+(NH_4^+):$2Cl^-$ Cotransport

In mouse MTAL cells ~45% of the initial rate of apical NH_4^+ entry occurred via the Ba^{2+}-sensitive pathway while 55% was mediated by Na^+:K^+(NH_4^+):$2Cl^-$ cotransport. Apical membranes of mouse MTAL cells also possess a Na^+:H^+ exchanger (Kikeri et al., 1990*a*); epithelial Na^+:H^+ exchangers can transport NH_4^+ (Kinsella and Aronson, 1981). However, the NH_4^+-induced acidification rate in S-MTAL was reduced by 98.5 ± 0.6% ($n = 7$) by the combination of Ba^{2+}, furosemide, and ouabain (compare segments c-d and b-g in Fig. 4, and segments c-d and b-f in Fig. 9). Moreover, the combination of luminal Ba^{2+} and furosemide in the IP-MTAL completely abolished the acidification observed on adding luminal NH_4^+ (Kikeri et al., 1989). Thus, the apical Na^+:H^+ exchanger in the mouse MTAL does not appear to mediate significant entry of NH_4^+ ions when compared with the entry attributable to the combination of the Ba^{2+}-sensitive pathway and the furosemide-sensitive cotransporter.

In the isolated perfused rat TAL, Good et al. (1984) found that luminal furosemide virtually abolished transepithelial NH_4^+ absorption. By contrast, in the rabbit TAL, furosemide inhibited only ~75% of active transcellular NH_4^+ flux (Garvin, Burg, and Knepper, 1985), indicating a role for a furosemide-independent apical NH_4^+ transport pathway. The apparent absence of furosemide-insensitive transepithelial NH_4^+

transport in the rat TAL may be due to species differences. Alternatively, the effects of paracellular and transcellular ammonium fluxes, as well as backfluxes from basolateral to apical solutions, may have obscured furosemide-insensitive NH_4^+ transport in studies of net transepithelial NH_4^+ transport. Thus, all species tested to date absorb NH_4^+ via the apical Na^+:K^+(NH_4^+):2Cl^- cotransporter, yet there may be considerable species differences in the role of the apical, barium-sensitive K^+(NH_4^+) pathway in NH_4^+ absorption (mouse > rabbit > rat).

The Ba^{2+}-sensitive NH_4^+ transport in MTAL: pH sensitivity and permeation via the apical K^+ channel. Fig. 14 *A* summarizes the effects of pH_i on the apical Ba^{2+}-sensitive

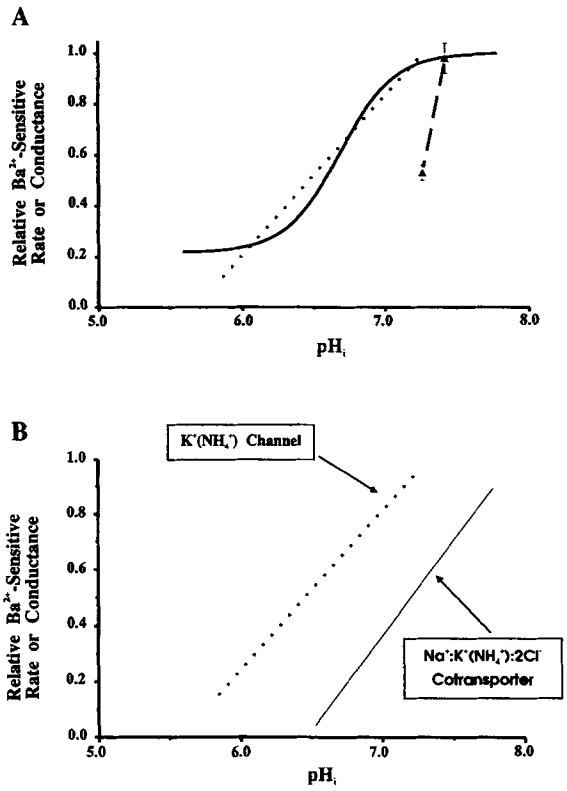

FIGURE 14. (*A*) Relationship between pH_i and relative, apical, Ba^{2+}-sensitive G_c (*solid line*), relative, apical, Ba^{2+}-sensitive N H_4^+ entry in IP-MTAL (*dotted line*), or relative, Ba^{2+}-sensitive NH_4^+ entry in S-MTAL (*dashed line*). (*B*) Relationship between pH_i and relative apical Ba^{2+}-sensitive NH_4^+ entry in IP-MTAL (*dotted line*), or relative apical NH_4^+ entry via Na^+:K^+/N H_4^+:2Cl^- (*solid line*) in IP-MTAL.

transcellular conductance (G_c; solid line) in IP-MTAL, the apical, Ba^{2+}-sensitive N H_4^+ transport pathway in IP-MTAL (dotted line), and the Ba^{2+}-sensitive NH_4^+ transport pathway in S-MTAL (dashed line; see below). In both S-MTAL and IP-MTAL preparations, J_{NH_4} was quite sensitive to pH_i changes over the physiological pH range 6–8. The finding that the pH_i-J_{NH_4} relationships obtained in IP-MTAL were similar (Fig. 8; dotted line in Fig. 14 *A*) whether pH_i was altered by basolateral pH_o or by luminal amiloride at constant apical and basolateral pH_o, indicated that the pH sensitivity of this Ba^{2+}-sensitive NH_4^+ transport pathway in IP-MTAL is cytosolic rather than extracellular.

The similarities of the effects of pH_i on G_c and the apical, Ba^{2+}-sensitive NH_4^+ influx suggests that both K^+ and NH_4^+ are being transported via the same or strikingly similar conductive pathways in apical membranes of MTAL cells. This possibility is supported by several recent observations. A Ba^{2+}-inhibitable K^+ channel with similar cytosolic pH sensitivity was observed by Bleich et al. (1990) in recent patch clamp studies of the apical membrane from in vitro perfused rat TAL segments. This was the only type of K^+ channel identified in apical membranes of rat TAL by these investigators, and the other observed properties of this channel indicated that it belonged to the class of ATP-regulated, inwardly rectifying K^+ channels (K_{ATP}). In fact, K_{ATP} channels with similar pH sensitivities have also been identified in patch clamp studies of principal cells from the rat renal cortical collecting duct (Wang et al., 1990), of early distal tubule cells from the kidney of *Rana pipens* (Hunter, Oberleithner, Henderson, and Giebisch, 1988; Wang, Henderson, Geibel, White, and Giebisch, 1989), and of B cells from the pancreatic islet (Rosario and Rojas, 1986*a*; Misler, Gillis, and Tabcharani, 1989). While Bleich et al. (1990) found that the K_{ATP} channel in apical membranes of rat TAL had similar permeabilities for K^+ and NH_4^+, they were unable to demonstrate any significant NH_4^+ current in cell excised patches (although this issue was not extensively evaluated in this study). Interestingly, the K_{ATP} channel found in pancreatic B cells does appear to exhibit a significant NH_4^+ permeability, the permeability ratio P_K:P_{NH_4}, estimated from fitting the *I-V* relations to the Goldman-Hodgkin-Katz equation, was 1:3 (Rosario and Rojas, 1986*b*). Finally, recent studies using site-directed mutagenesis of the *Drosophila* Shaker K^+ channel (although not a K_{ATP}-type channel) has demonstrated that certain mutations involving the H5 region, thought to line the channel pore (Guy and Conti, 1990; Yellen, Jurman, Abramson, and MacKinnon, 1991), significantly increased single channel NH_4^+ conductance (Yool and Schwarz, 1991). Thus it is possible that K^+ and NH_4^+ are being transported across apical membranes of the mouse MTAL via the same K_{ATP} channels.

From the curves shown in Fig. 14 *A*, it is also evident that the relative reduction in J_{NH_4} observed with decreasing pH_i in S-MTAL (Fig. 14 *A*, dashed line) was much steeper than that observed in the IP-MTAL (Fig. 14 *A*, solid and dotted lines). One or more of at least three factors may have accounted for the rightward shift of the J_{NH_4}–pH_i curve in S-MTAL. First, because basolateral membranes of MTAL cells are highly permeable to NH_3, $[NH_3]_i = [NH_3]_o$ in the presence of basolateral NH_4^+/NH_3, and consequently, $[NH_4^+]_i$ will increase with decreasing pH_i. pH_i-dependent increases in $[NH_4^+]_i$ would in turn reduce the electrochemical gradient for NH_4^+ entry, and thus, contribute to the pH_i-associated reduction of J_{NH_4} in S-MTAL. In contrast, $[NH_4^+]_i$ would not increase appreciably in IP-MTAL since basolateral medium did not contain NH_4^+. A second possible explanation for the rightward shift of the J_{NH_4}–pH_i curve in S-MTAL is that intracellular NH_4^+/NH_3 may have affected the activity of the Ba^{2+}-sensitive NH_4^+ transport pathway, independent of its effects on the NH_4^+ chemical gradient. While we know of no specific data addressing this issue for the K_{ATP} channel, a regulatory role for ammonium on another $K^+(NH_4^+)$ transporter has been suggested by other investigators (Kurtz and Balaban, 1986; Hamm, Gillespie, and Klahr, 1985). A third possible reason for the different pH_i sensitivities of the Ba^{2+}-sensitive NH_4^+ transport pathway in S-MTAL and IP-MTAL may be

related to differences in cytosolic ATP (or other as yet unknown cytosolic factors regulating K_{ATP} channels). In support of this possibility, Misler et al. (1989) found that the pH_i sensitivity of the K_{ATP} channel observed in cell-attached membrane patches of pancreatic B cells was essentially abolished in cell-detached, inside-out patches. Furthermore, exposure of the inside-out patches to small concentrations of ATP restored much of the pH sensitivity of these channels.

pH_i regulation of Na^+:$K^+(NH_4^+)$:2Cl^- cotransport. The apical Na^+:$K^+(NH_4^+)$:2Cl^- cotransporter mediated high rates of NH_4^+ entry into MTAL cells, in agreement with previous observations in TAL cells (Kinne et al., 1986; Garvin, Burg, and Knepper, 1988). NH_4^+ influx via Na^+:$K^+(NH_4^+)$:2Cl^- cotransport was sensitive to pH_i (Fig. 13). Paris and Pouysségur (1986) have shown previously that the activity of growth factor–activated Na^+:K^+:2Cl^- cotransport in fibroblasts was also reduced by cell acidification from ~7.5 to 6.5 pH units. Our observations are qualitatively similar. The mechanisms by which changes in pH_i alter Ba^{2+}-sensitive NH_4^+ transport and Na^+:$K^+(NH_4^+)$:2Cl^- cotransport are unknown.

TABLE I

Effect of Cell pH on Electrical Parameters of NaCl Transport in the Mouse MTAL

Buffer	pH_i	V_e	G_e	J_e
		mV	*mS · cm⁻²*	*pEq · s⁻¹ · cm⁻²*
HEPES	7.41 ± 0.02*	8.9 ± 1.5	123.4 ± 12.5‡	10,800 ± 1,700‡
CO_2/HCO_3^-	7.23 ± 0.02*	6.5 ± 1.3‡	119.5 ± 10.6‡	7,900 ± 1,900‡
P value	<0.001	<0.01	NS	<0.01

J_e = rate of net NaCl absorption calculated as $(V_e \cdot G_e)/F$.

*Data from Kikeri et al., 1990*a*.

‡Data from Hebert, 1987.

Fig. 14 *B* compares the pH_i sensitivity curves of the apical, Ba^{2+}-sensitive NH_4^+ transport pathway and the apical, furosemide-sensitive Na^+:$K^+(NH_4^+)$:2Cl^- cotransporter observed in the present IP-MAL studies. In the absence of basolateral/intracellular NH_4^+/NH_3, the pH_i sensitivity curve of Na^+:$K^+(NH_4^+)$:2Cl^- cotransport is located ~0.5 pH units to the right of the pH_i sensitivity curve of the apical Ba^{2+}-sensitive NH_4^+ transport pathway.

The differences in the pH_i sensitivities of the Na^+:$K^+(NH_4^+)$:2Cl^- cotransporter and $K^+(NH_4^+)$ channel observed in this study can explain our prior observation that switching from HEPES- to (CO_2/HCO_3^-)-buffered media diminished salt absorption in the mouse IP-MTAL (Hebert, 1987; Kikeri et al., 1990*a*). The pertinent results from these studies are summarized in Table I. Addition of CO_2/HCO_3^- to the external solutions bathing the IP-MAL resulted in a reduction in pH_i from 7.41 to 7.23. This cell acidification was associated with 17% decreases in V_e and the rate of NaCl absorption (J_e), but no significant change in G_e. These results are entirely consistent with the differences in the pH_i sensitivities of the two apical NH_4^+ transporters shown in Fig. 14 *B*. The arguments are as follows. If the (CO_2/HCO_3^-)-mediated fall in pH_i altered the apical cotransporter and not the apical $K^+(NH_4^+)$ channel, then the fall in

NaCl absorption should be quantitatively predicted by the pH_i sensitivity of the cotransporter. Using the pH_i titration equation fitted to the data in Figs. 13 and 14 *B*, the predicted rates of cotransporter activity would be 14.3 mM/min at pH_i 7.41 and 11.0 mM/min at pH_i 7.23, or a fall in cotransporter activity of ~13%, a value quite similar to the observed 17% fall in J_e. On the other hand, the lack of a significant change in G_e (Table I) is consistent with the lower pH_i sensitivity of the $K^+(NH_4^+)$ channel (Fig. 14 *B*).

Model of Effects of pH_i on Transcellular NH_4^+ Transport in MTAL

A model for the regulation of NH_4^+ transport, based on these and previous observations (Kikeri et al., 1989, 1990*a*), is presented in Fig. 15. Fig. 15 *A* shows the steady-state concentrations of extracellular and intracellular NH_4^+/NH_3 in MTAL cells in the presence of 5 mM ambient NH_4Cl (luminal/basolateral medium pH 7.4). Although apical membranes of mouse MTAL cells are virtually impermeable to NH_3, the concentrations of intracellular and basolateral (interstitial) NH_3 would be virtually equal since basolateral membranes of MTAL cells are highly permeable to NH_3 (Kikeri et al., 1989). Thus, the concentration of intracellular NH_4^+ will depend on the pH_i and the NH_3 concentration of the basolateral medium. For this example the steady-state pH_i in the presence of 5 mM ambient NH_4Cl would be 7.13. Fig. 15 *B* depicts the effects of both NH_4^+-induced pH_i changes and intracellular NH_4^+/NH_3 on transcellular NH_4^+ transport in the mouse MTAL in the presence of ambient 5 mM NH_4Cl. NH_4^+ entry from the lumen would result in the net generation of H^+ with NH_3 diffusing down its gradient into the medullary interstitium. Because of the negligible apical membrane NH_3 permeability, NH_3 backleak from the cytoplasm to the lumen would be minimal (Kikeri et al., 1989). Because of the large cellular buffering power, B_t, most of the H^+ load due to NH_4^+ entry would be buffered, thus attenuating the drop in pH_i. The increasing B_t with acidification below a pH of 7.0 (Fig. 2) would also help to attenuate pH_i changes resulting from apical NH_4^+ entry. Nevertheless, cell acidification due to NH_4^+ entry would (*a*) inhibit NH_4^+ entry via the apical entry pathways, and (*b*) increase the rate of apical (Kikeri et al., 1990*a*) and basolateral (Sun and Hebert, 1990) $Na^+:H^+$ exchange. The combined effect of reduced NH_4^+ entry and increased $Na^+:H^+$ exchange would result in an increase in pH_i, which would tend to restore NH_4^+ entry via the apical entry pathways and decrease the rate of $Na^+:H^+$ exchange. At the steady-state pH_i in the presence of 5 mM ambient NH_4Cl (7.13 pH units), H^+ influx due to NH_4^+ entry would be balanced by H^+ efflux (predominantly via $Na^+:H^+$ exchange) due to NH_4^+ exit (Fig. 5).

Some Physiological Implications of This Model for NH_4^+ and NaCl Transport

Changes in pH_i in the presence of basolateral/intracellular NH_4^+/NH_3 may affect the rate of apical NH_4^+ transport by altering the NH_4^+ chemical gradient. Thus, the concentration of NH_3 in the medullary interstitium surrounding the MTAL may play an important role in regulating transcellular NH_4^+ absorption by the in vivo MTAL; the rate of transcellular NH_4^+ flux would be high in the presence of low interstitial NH_3 concentrations and vice versa. In other words, as the medullary interstitial concentration of NH_4^+/NH_3 rises, transcellular NH_4^+ transport would be inhibited because of an increase in intracellular NH_4^+/NH_3 concentrations. The inhibitory effect

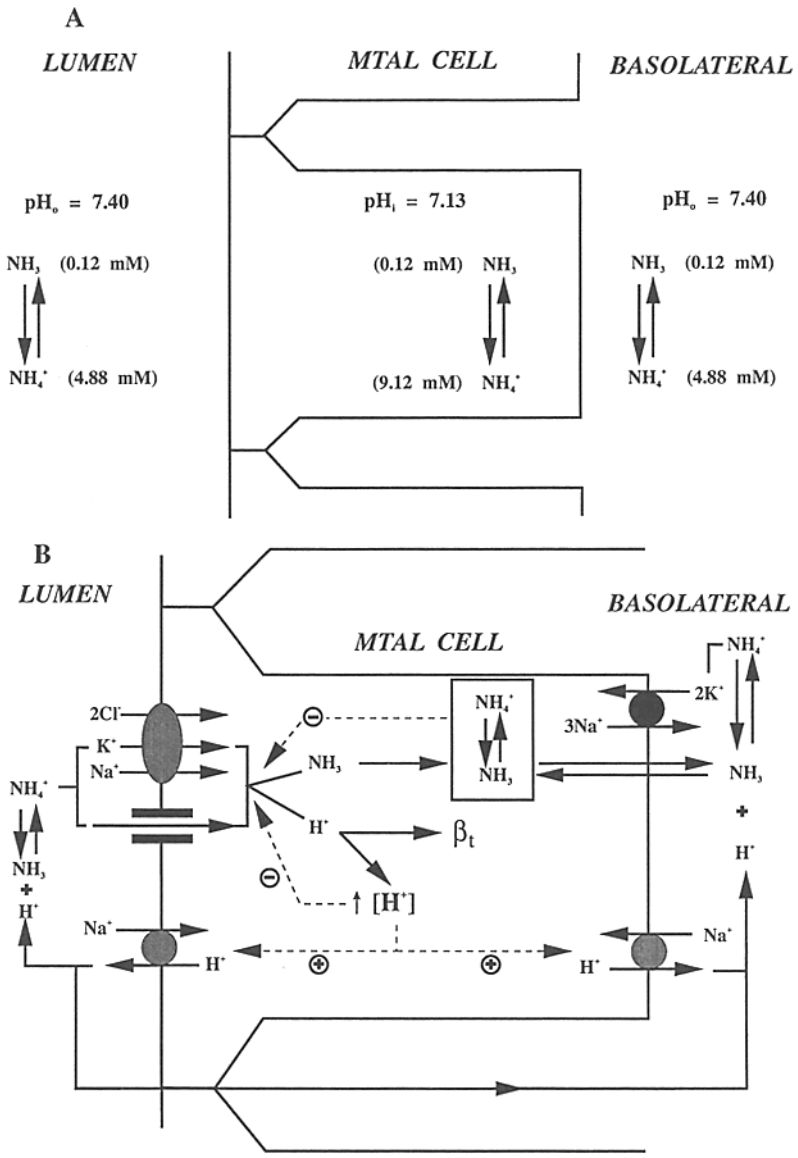

FIGURE 15. (*A*) Steady-state intracellular and extracellular concentrations of NH_4^+/NH_3 in the nominal presence of 5 mM NH_4Cl in both apical and basolateral media (pH$_o$ 7.40) at pH$_i$ 7.13. The pKa for ammonium was 9.0. (*B*) Model of role of pH$_i$ and NH_4^+/NH_3 in regulating transcellular NH_4^+ transport in the mouse MTAL. The single arrow showing apical NH_4^+ entry represents NH_4^+ entry via both the apical, Ba^{2+}-sensitive NH_4^+ pathway and the apical, Na^+:K^+/NH_4^+:$2Cl^-$ pathway. See text for detailed discussion.

of intracellular NH_4^+/NH_3 on transcellular NH_4^+ transport could be due to either a reduction in the NH_4^+ chemical gradient or an effect (either directly or indirectly) of intracellular NH_4^+/NH_3 on the apical NH_4^+ transport pathways. This "negative feedback loop" would limit the maximum interstitial concentrations of NH_4^+/NH_3, which in turn is believed to play an important role in regulating renal NH_4^+ excretion (Knepper et al., 1989).

NaCl reabsorption by the MTAL both dilutes the urine and provides the single effect of the countercurrent multiplication process which is required for vasopressin-dependent concentration of urine in the medullary collecting duct. Net NaCl absorption by the mouse MTAL is dependent on the activities of both the apical $Na^+:K^+:2Cl^-$ cotransporter and the apical K^+ channel (Hebert and Andreoli, 1986). Given the results of this study, it seems reasonable to speculate that the pH_i and/or the presence of basolateral/intracellular NH_4^+/NH_3 may affect the rate of transepithelial NaCl absorption in the mouse MTAL by altering the activities of both of these ion transporters. Several lines of evidence support this possibility. First, as discussed above, the results in Table I are consistent with this notion. Second, Wingo (1986) has demonstrated that both respiratory and metabolic acidosis result in a reduction of transepithelial Cl^- transport in the TAL. Since both an increase in ambient CO_2 concentration (Kikeri et al., 1990*a*) and metabolic acidosis would be expected to lead to cell acidification, inhibition of apical ion transport pathways in the TAL by cell acidification may explain the acidosis-induced reduction of transepithelial Cl^- absorption observed by Wingo (1986). Third, the MTAL in the isolated perfused rat kidney is exquisitely vulnerable to hypoxic injury (Brezis, Rosen, Silva, and Epstein, 1984*a*) because of the high rates of transport-related energy consumption by the MTAL (measured as ouabain-sensitive oxygen consumption [Brezis, Rosen, Silva, and Epstein, 1984*b*]). Reduction of the perfusate pH (acidosis) markedly attenuates hypoxic injury to MTAL in the isolated perfused rat kidney (Shanley, Shapiro, Chan, Burke, and Johnson, 1988). An attractive explanation for the acidosis-induced protection against hypoxic MTAL cell injury is that inhibition of ion transport-dependent oxygen consumption in the MTAL (>50% of total oxygen consumption [Kirkeri et al., 1990*a*]) by cell acidification may protect against cell damage in hypoxic conditions. Fourth, it has long been recognized that the oral administration of an NH_4Cl load leads to diuresis, natriuresis, and kaliuresis without a consistent change in glomerular filtration rate (Pitts, 1959; Sartorius, Roemmelt, and Pitts, 1949). Inhibition of apical ion transporters in the TAL and possibly in other nephron segments by NH_4^+-induced cell acidification or by intracellular NH_4^+/NH_3 itself may at least partially explain the effects of acute NH_4Cl loading on salt and H_2O excretion by the kidney. Finally, alterations in pH_i have been suggested to alter transport processes in diluting segments. Weigt, Dietl, Silbernagl, and Oberleithner (1987) and Wang et al. (1989) have suggested that the effect of aldosterone on the apical K^+ channel in the frog diluting segment is mediated by cell alkalinization due to activation of $Na^+:H^+$ exchange.

Technical support was provided by M. Lombardi.

D. Kikeri and A. Sun are recipients of individual National Research Service Awards from the NIH (DK-08160 and DK-08039, respectively). M. L. Zeidel is the recipient of Research Career Develop-

ment and Merit Review awards from the Department of Veterans Affairs. This study was supported by grants to M. L. Zeidel (DK-38690 and the Harvard Center for the Study of Kidney Disease, 1 P50 DK-39249, project 3) and an NIH grant to S. C. Hebert (DK-37605).

Original version received 9 August 1991 and accepted version received 19 November 1991.

REFERENCES

Aickin, C. C. 1984. Direct measurement of intracellular pH and buffering power in smooth muscle cells of guinea-pig vas deferens. *Journal of Physiology.* 349:571–585.

Bleich, M., E. Schlatter, and R. Greger. 1990. The luminal K^+ channel of the thick ascending limb of Henle's loop. *Pflügers Archiv.* 415:449–460.

Boyarsky, G., M. B. Ganz, R. B. Sterzel, and W. F. Boron. 1988. pH regulation in single glomerular mesangial cells. I. Acid extrusion in absence and presence of HCO_3^-. *American Journal of Physiology (Cell Physiology).* 255:C844–C856.

Brezis, M., S. Rosen, P. Silva, and F. H. Epstein. 1984*a*. Selective vulnerability of the medullary thick ascending limb to anoxia in the isolated perfused rat kidney. *Journal of Clinical Investigation.* 73:182–190.

Brezis, M., S. Rosen, P. Silva, and F. H. Epstein. 1984*b*. Transport activity modifies thick ascending limb damage in the isolated perfused kidney. *Kidney International.* 25:65–72.

Brown, D., S. Hirsch, and S. Gluck. 1988. Localization of a proton-pumping ATPase in rat kidney. *Journal of Clinical Investigation.* 82:2114–2126.

Garvin, J. L., M. B. Burg, and M. A. Knepper. 1985. Ammonia replaces potassium in supporting sodium transport by the Na-K-ATPase of renal proximal straight tubules. *American Journal of Physiology (Renal Fluid Electrolyte Physiology 18).* 249:F785–F788.

Garvin, J. L., M. B. Burg, and M. A. Knepper. 1988. Active NH_4^+ absorption by the thick ascending limb. *American Journal of Physiology (Renal Fluid Electrolyte Physiology 24).* 255:F57–F65.

Good, D. W., and M. B. Burg. 1984. Ammonia production by individual segments of the rat nephron. *Journal of Clinical Investigation.* 73:602–610.

Good, D. W., M. A. Knepper, and M. B. Burg. 1984. Ammonia and bicarbonate transport by the thick ascending limb of the rat. *American Journal of Physiology (Renal Fluid Electrolyte Physiology).* 247:F35–F44.

Grinstein, S., and W. Furuya. 1986. Characterization of the Na^+-H^+ antiport of human neutrophils. *American Journal of Physiology. (Cell Physiology).* 250:C283–C291.

Guy, H. R., and F. Conti. 1990. Pursuing the structure and function of voltage-gated channels. *Trends in Neurological Sciences.* 13:201–206.

Hamm, L. L., C. Gillespie, and S. Klahr. 1985. NH_4Cl inhibition of transport in the rabbit cortical collecting tubule. *American Journal of Physiology (Renal Fluid Electrolyte Physiology).* 248:F631–F637.

Hebert, S. C. 1986. Hypertonic cell volume regulation in mouse thick limbs I. ADH dependency and nephron heterogeneity. *American Journal of Physiology (Cell Physiology).* 250:C907–C919.

Hebert, S. C. 1987. Volume regulation in renal epithelial cells. *Seminars in Nephrology.* 7:48–60.

Hebert, S. C., and T. E. Andreoli. 1984. Effects of antidiuretic hormone on cellular conductive pathways in mouse medullary thick ascending limbs of Henle: II. Determinants of the ADH-mediated increases in transepithelial voltage and in net Cl absorption. *Journal of Membrane Biology.* 80:221–233.

Hebert, S. C., and T. E. Andreoli. 1986. Ionic conductance pathways in the mouse medullary thick ascending limb of Henle. The paracellular pathway and electrogenic Cl^- absorption. *Journal of General Physiology.* 87:567–590.

Hebert, S. C., R. M. Culpepper, and T. E. Andreoli. 1981*a*. NaCl transport in mouse medullary thick ascending limbs. I. Functional nephron heterogeneity and ADH-stimulated NaCl cotransport. *American Journal of Physiology (Renal Fluid Electrolyte Physiology).* 241:F412–F431.

Hebert, S. C., R. M. Culpepper, and T. E. Andreoli. 1981*b*. NaCl transport in mouse medullary thick ascending limbs II. ADH enhancement of transcellular NaCl cotransport; origin of the transepithelial voltage. *American Journal of Physiology (Renal Fluid Electrolyte Physiology).* 241:F432–F442.

Hebert, S. C., P. A. Friedman, and T. E. Andreoli. 1984. Effects of antidiuretic hormone on cellular conductive pathways in mouse medullary thick ascending limbs of Henle: I. ADH increases transcellular conductive pathways. *Journal of Membrane Biology.* 80:201–219.

Hebert, S. C., and A. M. Sun. 1991. Rapid cell volume regulation on the mouse medullary thick ascending limb of Henle. Nephrology. Vol. 1. M. Hatano, editor. Springer-Verlag, Tokyo. 630–640.

Hunter, M., H. Oberleithner, R. M. Henderson, and G. Giebisch. 1988. Whole-cell potassium currents in single early distal tubule cells. *American Journal of Physiology (Renal Fluid Electrolyte Physiology 24).* 255:F699–F703.

Kikeri, D., S. Azar, A. Sun, M. L. Zeidel, and S. C. Hebert. 1990*a*. Na^+-H^+ antiporter and Na^+-$(HCO_3^-)_n$ symporter regulate intracellular pH in mouse medullary thick limbs of Henle. *American Journal of Physiology (Renal Fluid Electrolyte Physiology 27).* 258:F445–F456.

Kikeri, D., A. Sun, M. L. Zeidel, and S. C. Hebert. 1989. Cell membranes impermeable to NH_3. *Nature.* 339:478–480.

Kikeri, D., M. L. Zeidel, B. J. Ballermann, B. M. Brenner, and S. C. Hebert. 1990*b*. pH regulation and response to AVP in A10 cells differ markedly in the presence vs. absence of CO_2-HCO_3^-. *American Journal of Physiology (Cell Physiology 28).* 259:C471–C483.

Kinne, R., E. Kinne-Saffran, H. Schuetz, and B. Schloelermann. 1986. Ammonia transport in medullary thick ascending limb of rabbit kidney: involvement of the Na^+, K^+, Cl^--cotransporter. *Journal of Membrane Biology.* 94:279–284.

Kinsella, J. L., and P. S. Aronson. 1981. Interaction of NH_4^+ and Li^+ with the renal microvillus membrane Na^+-H^+ exchanger. *American Journal of Physiology (Cell Physiology 10).* 241:C220–C226.

Knepper, M. A., R. Packer, and D. W. Good. 1989. Ammonium transport in the kidney. *Physiological Reviews.* 69:179–249.

Krapf, R., R. J. Alpern, F. C. Rector, Jr., and C. A. Berry. 1987. Basolateral membrane Na/base cotransport is dependent on CO_2/HCO_3 in the proximal tubule. *Journal of General Physiology.* 90:833–853.

Kurtz, I., and R. S. Balaban. 1986. Ammonium as a substrate for Na^+-K^+-ATPase in rabbit proximal tubules. *American Journal of Physiology (Renal Fluid Electrolyte Physiology 19).* 250:F497–F502.

Misler, S., K. Gillis, and J. Tabcharani. 1989. Modulation of gating of a metabolically regulated, ATP-dependent K^+ channel by intracellular pH in B cells of the pancreatic islet. *Journal of Membrane Biology.* 109:135–143.

Molony, D. A., and T. E. Andreoli. 1988. Diluting power of thick limbs of Henle: I. Peritubular hypertonicity blocks basolateral Cl^- channels. *American Journal of Physiology (Renal Fluid Electrolyte Physiology).* 255:F1128–F1137.

Nagami, G. T., and K. Kurokawa. 1985. Regulation of ammonia production by mouse proximal tubules perfused in vitro. Effect of luminal perfusion. *Journal of Clinical Investigation.* 75:844–849.

Oberleithner, H., G. Munich, A. Schwab, and P. Dietl. 1986. Amiloride reduces potassium conductance in frog kidney via inhibition of Na^+-H^+ exchange. *American Journal of Physiology (Renal Fluid Electrolyte Physiology).* 251:F66–F73.

Paris, S., and J. Pouysségur. 1986. Growth factors activate the bumetanide-sensitive $Na^+/K^+/Cl^-$ cotransport in hamster fibroblasts. *Journal of Biological Chemistry.* 261:6177–6183.

Pitts, R. F. 1959. Acidifying agents: ammonium chloride. *In* The Physiological Basis of Diuretic Therapy. R. F. Pitts, editor. Charles C. Thomas, Springfield, IL. 158–167.

Roos, A., and W. F. Boron. 1981. Intracellular pH. Physiological Reviews. 61:296–434.

Rosario, L. M., and E. Rojas. 1986*a*. Modulation of K^+ conductance by intracellular pH in pancreatic β-cells. *FEBS Letters.* 200:203–208.

Rosario, L. M., and E. Rojas. 1986*b*. Potassium channel selectivity in mouse pancreatic B cells. *American Journal of Physiology (Cell Physiology 19).* 250:C90–C94.

Sartorius, O. W., J. C. Roemmelt, and R. F. Pitts. 1949. The renal regulation of acid-base balance in man. IV. The nature of the renal compensations in ammonium chloride acidosis. *Journal of Clinical Investigation.* 28:423–439.

Shanley, P. F., J. I. Shapiro, L. Chan, T. J. Burke, and G. C. Johnson. 1988. Acidosis and hypoxic medullary injury in the isolated perfused kidney. *Kidney International.* 34:791–796.

Sun, A., and S. C. Hebert. 1990. Rapid cell volume regulation by the mouse medullary thick ascending limb of Henle. *Proceedings of the XI International Congress of Nephrology.* H. Michinobu, editor. Springer-Verlag, Tokyo.

Thomas, J. A., R. N. Buchsbaum, A. Zimniak, and E. Racker. 1979. Intracellular pH measurements in Ehrlich ascites tumor cells utilizing spectroscopic probes generated in situ. *Biochemistry.* 18:2210–2218.

Wang, W., R. M. Henderson, J. Geibel, S. White, and G. Giebisch. 1989. Mechanism of aldosterone-induced increase of K^+ conductance in early distal renal tubule cells of the frog. *Journal of Membrane Biology.* 111:277–289.

Wang, W., S. White, J. Geibel, and G. Giebisch. 1990. A potassium channel in the apical membrane of rabbit thick ascending limb of Henle's loop. *American Journal of Physiology (Renal Fluid Electrolyte Physiology 27).* 258:F244–F253.

Weigt, M., P. Dietl, S. Silbernagl, and H. Oberleithner. 1987. Activation of luminal Na^+/H^+ exchange in distal nephron of frog kidney: an early response to aldosterone. *Pflugers Archiv.* 408:609–614.

Wingo, C. S. 1986. Effect of acidosis on chloride transport in the cortical thick ascending limb of Henle perfused in vitro. *Journal of Clinical Investigation.* 78:1324–1330.

Yellen, G., M. E. Jurman, T. Abramson, and R. Mackinnon. 1991. Mutations affecting internal TEA blockade identify the probable pore-forming region of a K^+ channel. *Science.* 251:939–942.

Yool, A. J., and T. L. Schwarz. 1991. Alteration of ionic selectivity of a K^+ channel by mutation of the H5 region. *Nature.* 349:700–704.

Zeidel, M. L., P. Silva, and J. L. Seifter. 1986. Intracellular pH regulation and proton transport by renal medullary collecting duct cells. Role of plasma membrane proton adenosine triphosphatase. *Journal of Clinical Investigation.* 77:113–120.